ARTICLE

Molecular Diagnostics

# The tumour-associated stroma correlates with poor clinical outcomes and immunoevasive contexture in patients with upper tract urothelial carcinoma: results from a multicenter real-world study (TSU-01 Study)

Longhao Xu[1,8], Wenlong Zhong[1,8], Chenchen Li[2,8], Peng Hong[3,8], Kun Xia[1,4], Rongcheng Lin[5], Sida Cheng[6], Bo Wang[1], Meng Yang[7], Junyu Chen[1], Lulin Ma[3], Xuesong Li[6]✉, Liqun Zhou[6]✉, Jian Huang[1]✉ and Tianxin Lin[1]✉



**BACKGROUND:** In this real-world study, we aimed to elucidate the predictive value of tumour-associated stroma for clinical prognostic and therapeutic response in upper tract urothelial carcinoma (UTUC) by reviewing the clinicopathologic characteristics of 1015 UTUC patients through a nationwide multicenter analysis.

**METHODS:** The tumour–stroma ratio (TSR) was assessed based on tissue sections stained for hematoxylin and eosin (H&E), and patients were further stratified into stroma-high (>50% stroma) and stroma-low group (≤50% stroma). Kaplan–Meier curve and Cox regression hazard analysis were conducted to assess the survival outcomes of UTUC patients. Bioinformatics analysis and immunostaining analysis were applied to portray the tumour microenvironment (TME).

**RESULTS:** Stroma-high UTUC was significantly associated with poorer survival outcomes and inferior chemotherapeutic responsiveness. Our established nomogram achieved a high prognostic accuracy in predicting overall survival and cancer-specific survival in both of the discovery cohort (area under the curve [AUC] 0.663 and 0.712) and the validation cohort (AUC 0.741 and 0.747). Moreover, stroma-high UTUC was correlated with immunoevasive TME accompanied by increased cancer-associated fibroblasts, tumour-associated macrophages and, conspicuously a cluster of highly exhausted $CD8^+$ T cells.

**CONCLUSION:** Our results showed stroma-high UTUC was associated with an inferior prognosis and an immunoevasive TME with exhausted $CD8^+$ T cells in UTUC patients. Our TSR-based nomogram could be used to refine prognosis and inform treatment decisions of patients with UTUC.

*British Journal of Cancer* (2023) 128:310–320; https://doi.org/10.1038/s41416-022-02049-1

## INTRODUCTION

Malignancy of the upper urinary tract is a relatively rare and diverse group of tumours, accounting for roughly 5–10% of all urothelial carcinomas [1]. Upper tract urothelial carcinoma (UTUC) is characterised by a distinctly aggressive clinical phenotype, with a poorer stage-for-stage prognosis than bladder urothelial carcinomas [2, 3]. Currently, risk stratification in UTUC is based largely on the tumour–node–metastasis (TNM) staging guidelines set forth in the American Joint Committee on Cancer (AJCC) staging systems [4, 5]. Although this anatomy-based system provides useful information, UTUCs in the same stage may still have significant differences in prognosis. On the other hand, due to the similar pathological features of UTUC and urothelial carcinoma of the bladder, adjuvant chemotherapy (ACT) is commonly used for locally advanced UTUC. However, current findings on the application of ACT for UTUC are controversial [6–8]. Thus, there is an urgent need to improve the accuracy of risk stratification and precisely identify those patients who might benefit most from ACT.

Given the low incidence of UTUC, data on new prognostic and predictive biomarkers are sparse, and the existing studies mainly focus on intrinsic properties of tumour cells [3, 9, 10]. Regardless of

[1]Department of Urology, Sun Yat-sen Memorial Hospital; Guangdong Provincial Key Laboratory of Malignant Tumor Epigenetics and Gene Regulation; Guangdong Provincial Clinical Research Center for Urological Diseases, Sun Yat-sen (Zhongshan) University, Guangzhou, P. R. China. [2]Department of Medical Oncology, The Sixth Affiliated Hospital, Sun Yat-sen University, Guangzhou, P. R. China. [3]Department of Urology, Peking University Third Hospital, Beijing, P. R. China. [4]Department of Urology, Jiangxi provincial People's Hospital Affiliated to Nanchang University, Nanchang, P. R. China. [5]Department of Urology, Fujian Provincial Hospital, Fuzhou, P. R. China. [6]Department of Urology, Peking University First Hospital, Beijing, P. R. China. [7]Department of Urology, Yan'an Hospital Affiliated with Kunming Medical University, Kunming, P. R. China. [8]These authors contributed equally: Longhao Xu, Wenlong Zhong, Chenchen Li, Peng Hong. ✉email: pineneedle@sina.com; zhoulqmail@sina.com; huangj8@mail.sysu.edu.cn; lintx@mail.sysu.edu.cn

Received: 2 May 2022 Revised: 23 September 2022 Accepted: 27 October 2022
Published online: 17 November 2022

the promising results of these biomarkers, their applicability has been jeopardised due to their limited clinical value. Though an appreciation for the role of the tumour microenvironment (TME) in prognostic prediction is emerging, insufficient attention is paid to the underlying TME heterogeneity of UTUCs. Currently, accumulating evidence has suggested that tumour-associated stroma may contribute to the development, progression and metastasis of cancer [11–13]. The tumour–stroma ratio (TSR), which estimates the amount of stromal proliferation within the borders of the tumour, was identified as a strong prognostic indicator and possible predictor of chemotherapy benefit in several types of cancers [14–17]. Based on the histological analysis of hematoxylin and eosin (H&E)-stained paraffin sections, TSR appeared to be sufficiently robust and could be easily implemented in routine clinical applications [14, 15].

Different components of the TME might be useful indicators for predicting cancer survival, as well as chemotherapy benefits in various types of solid tumours [10, 18, 19]. Indeed, tumour stroma may have an influence on immune cells recruitment and activation, and the TSR has been reported to reflect the status of the TME [20]. Tumour–stroma can prevent the infiltration of effector immune cells and promote the recruitment of immunosuppressive cells to the TME, which ultimately affect the development of tumours [20]. However, to the best of our knowledge, no large-scale, multicenter studies have been performed to investigate the role of TSR in patients with UTUC to date.

In this study, the primary aim of this study was to evaluate the prognostic and predictive role of the TSR in UTUC through a nationwide multicenter analysis comprising over 1,000 patients. The secondary aim was to investigate the underlying mechanisms of tumour–stroma interaction in the TME of UTUCs.

## METHODS

### Study design

This study, namely tumour–stroma signatures of UTUC (TSU-01), is a nationwide multicenter, real-world study promoted by the Chinese Urology Doctors' Association (CUDA)-UTUC Collaborative Group. A total of 1015 patients who underwent radical nephroureterectomy (RNU) for UTUC at four Chinese Institutions (Sun Yat-sen Memorial Hospital, Guangzhou; Peking University First Hospital, Beijing; Peking University Third Hospital, Beijing and Fujian Provincial Hospital, Fujian), between January 1, 2006 and December 31, 2017, were included in this study. Exclusion criteria were patients with metastatic disease at diagnosis, without available H&E slides or complete follow-up information. The enrolled patients were divided into the discovery cohort and the validation cohort by simple random sampling, with a random number seed of 2,017,0307 [21]. In addition, RNA sequencing (RNA-Seq) cohort enrolled additional 29 UTUC patients from Peking University First Hospital. For sample selection, consecutive consenting patients who underwent radical nephroureterectomy (RNU) for UTUC at Peking University First Hospital between January 2017 and December 2017 were enrolled in this study. In addition, the specimens were collected from consecutive patients after surgery, and only samples that met the requirements of histopathological diagnosis and were of high enough quality for RNA sequencing were used. The pathological staging was determined according to the 8th AJCC TNM classification, and tumour grading was performed according to the 2004 World Health Organisation classification. Clinicopathological data, including sex, age at surgery, tumour characteristics, and treatment-related variables, were retrospectively collected. A flowchart summarising the study selection procedure is presented in Fig. 1.

### Outcomes

The main outcome of this study was overall survival (OS), defined as the time interval between surgery and death from any case. The secondary outcome was cancer-specific survival (CSS), defined as the time from the date of the first surgery to the date of death caused by UTUC.

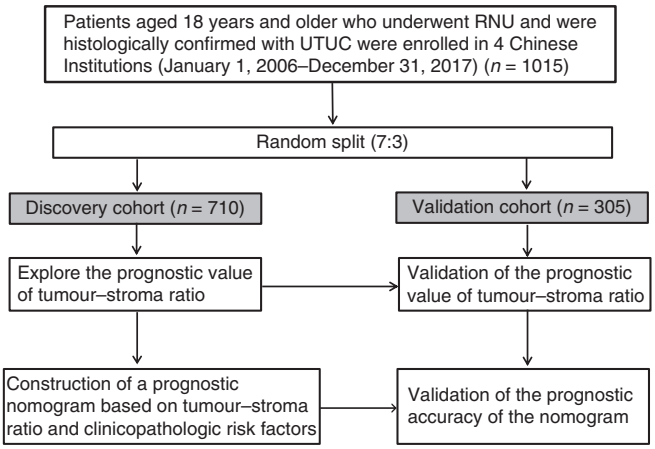


**Fig. 1 Flowchart of the study.** A total of 1015 patients meeting the inclusion/exclusion criteria were included. RNU Radical nephroureterectomy, UTUC Upper tract urothelial carcinoma.

### The evaluation of the TSR

Evaluation of the TSR in UTUC tissues was performed on 4 μm H&E-stained sections as previously described [14–16]. Briefly, the full-face sections were scanned using conventional microscopy, and H&E sections from the deepest point of tumour invasion were selected. From this section, areas with the highest amount of stroma were selected using a 10× objective. Subsequently, the TSR was visually evaluated using a ×10 objective within an area where both tumour cells and their surrounding stromal tissue were present. Tumour cells must be present at all four borders of the selected image field. Areas of necrosis, haemorrhage and smooth muscle tissue were excluded. The TSR was analysed in increments of ten percentage points (10, 20, 30%, etc.) (Supplementary Fig. S1). Tumours were classified as stroma-high subgroup (>50% stromal area) and stroma-low subgroup (≤50% stromal area), as previously reported by Huijbers et al. [14–16]. To assess the concordance between pathologists in the TSR assessment, 2 independent investigators (PH and WLZ) blinded to clinicopathological data and patient outcomes conducted the evaluation, with a concordance of classification of 94% (Cohen's kappa = 0.906). Any disagreements were resolved by consensus after consultation between the investigators and a senior pathologist.

### Immunohistochemistry and evaluation

For the evaluation of IHC, we collected tumour tissues from 91 patients who underwent radical nephroureterectomy (RNU) for UTUC from Sun Yat-sen Memorial Hospital from January 2015 to December 2017. All enrolled patients signed informed consent. Exclusion criteria were patients with metastatic disease at diagnosis, without available H&E slides or complete follow-up information. Immunohistochemistry (IHC) analysis of the expression of CD4, CD8, FOXP3, CD68, CD206, CD66b, CD20 and α-SMA was performed. Detailed information of the antibodies for IHC analysis is shown in Supplementary Table S1.

As previously reported in the literature [22–24], whole slides were dewaxed in xylene, rehydrated in a series of graded alcohols. Then, after antigen repair, inactivation of endogenous peroxidase, and blocking of non-specific binding sites, slides were incubated with primary antibodies overnight at 4 °C. Afterwards, the slides were incubated with the Dako REAL™ EnVision™/horse radish peroxidase (HRP), Rabbit/Mouse detection reagent for 30 min. Eventually, the slides were incubated with the buffered hydrogen peroxide diaminobenzidine chromogen solution (REAL™ DAB$^+$ Chromogen/REAL™ Substrate Buffer; Dako), and then counterstained with hematoxylin.

Two investigators, who were blinded to the clinical outcome, independently evaluated the IHC analysis outcome. The densities of immune cells in the intratumoral and stromal regions of all samples were screened at low power magnification (×100 magnification), and then the five most representative fields were selected and examined at high-power magnification (×400 magnification) (0.07 mm$^2$ per field). The cells were counted using an ImageJ cell-counter plugin, and counts were subsequently converted into densities (cells/field). Any differences were resolved through consensus between two investigators and a senior pathologist.

### Multiplexed immunofluorescence staining and evaluation

Multiplexed immunofluorescence (mIF) staining was performed using the PANO 4-plex IHC kit (Panovue, Beijing, China), according to the manufacturer's protocol, to visualise the expression of CD8, PD-1, VISTA, TIM-3 and LAG-3 (Supplementary Table S1). Briefly, each paraffin-embedded sample was deparaffinized and rehydrated. The slides were subjected to antigen retrieval buffer treatment performed by microwave treatment after blocking the endogenous peroxide activity. The slides were then incubated with the corresponding primary antibody overnight at 4 °C. Subsequently, after washing, the slides were incubated for 10 min with HRP-conjugated secondary antibody and enhanced by the tyramide signal amplification method. For each additional marker, the protocol was repeated by treating the slides with an antigen retrieval step, followed by the corresponding primary antibody staining and the subsequent downstream steps. Finally, nuclei were stained with 4′,6-diamidino-2-phenylindole (DAPI) after all the antigens had been labelled.

For the evaluation of mIF, each mIF image was analysed using the InForm software (InForm™, PerkinElmer). Briefly, each immune cell biomarker antibody was paired with an individual Opal fluorophore (Panel1: CD8-Opal 520, TIM-3-Opal 570, LAG-3-Opal 690; Panel2: CD8-Opal 520, PD-1-Opal 570, VISTA-Opal 690), and a built-in algorithm was used to segment tumour and non-tumour regions by training the software on a limited number of regions. Cell segmentation was performed based on DAPI staining of nuclei. The cells in the tumoral and stromal region were phenotyped and counted by training the inForm software to recognise each cell type. Subsequent analysis was performed using inForm's exported cell positional data.

### RNA sequencing and data analysis

The detailed clinicopathological characteristics of the enrolled patients are listed in Supplementary Table S2. The data were transformed to FPKM (fragments per kilobase of exon per million fragments mapped) and HTSeq-count before statistical analysis. The microenvironment cell populations counter (MCP-counter), a transcriptome-based computational method, was used for directly compare the relative abundance of eight immune cells and two stromal cell populations in tissues [25], as described by Becht et al. [26]. Differentially expressed genes were obtained by using DESeq2 with filtering parameters of fold change above 2, adjusted $P < 0.05$ [27]. Gene Set Enrichment Analysis (GSEA) was performed to investigate the upregulated and downregulated functions of genes that significantly correlated to tumour-associated stroma [28]. The involved immune cell gene sets and other immune-related signatures were reported from previous studies [29, 30] (Supplementary Table S3).

### Statistical analysis

Categorical data were analysed using Pearson's chi-squared test. Continuous data were evaluated using the Mann–Whitney *U*-test. Weighted κ statistic was used to evaluate the interrater agreement for the TSR measurement. The Kaplan–Meier log-rank analysis was used to estimate OS and CSS. Univariable and multivariable Cox models were used to calculate hazard ratios (HRs) and 95% confidence intervals (95% CI). The time-dependent receiver operating characteristic (ROC) curve and the area under the curve (AUC) at 5 years were used to determine the prognostic accuracy. In the subgroup analysis, propensity score matching (PSM) was performed to balance the groups. Patients treated with ACT were matched 1:4 with patients not treated with ACT using nearest neighbour matching with a calliper of 0.2. All analyses were conducted using the R software (version 4.0.2) and GraphPad Prism 8 software (GraphPad Software Inc, San Diego, CA, USA). Statistical significance *P* value was set at 0.05 with two sides.

## RESULTS

### Clinicopathological characteristics of patients

In total, 710 patients (361 males [50.8%] and 349 females [49.2%]) were included in the discovery cohort, and 305 patients (153 males [50.2%] and 152 females [49.8%]) were included in the validation cohort. The detailed baseline clinical characteristics of the enrolled UTUC patients were listed in Table 1. In the discovery cohort, 61.4% ($n = 436$) patients were categorised as the stroma-low group and 38.6% ($n = 274$) as the stroma-high group. Similarly, there were 61.0% ($n = 186$) stroma-low patients and 39.0% ($n = 119$) stroma-high patients in the validation cohort. Noteworthily, stroma-high group significantly correlated with higher pathological grade and poorer TNM stage in both cohorts (discovery cohort, both $P < 0.001$; validation cohort, both $P < 0.001$) (Table 1).

### A higher TSR indicates poorer clinical outcomes in patients with UTUC

The median follow-up time was 42 (interquartile range 22.0−64.0) months for all the patients. During follow-up, 242 patients (23.8%) died from all causes, and 179 patients (17.6%) died from UTUC at the time of data analysis. The 5-year OS was 74.1% for stroma-high tumours vs. 84.4% for stroma-low tumours in the discovery cohort (OS: $P < 0.0001$; Fig. 2a). Similarly, stroma-high patients had significantly shorter CSS compared to stroma-low patients in the discovery cohort (CSS: $P < 0.0001$; Fig. 2b). Consistently, the 5-year OS and CSS was lower among stroma-high tumours than among stroma-low tumours in the validation cohort (OS: $P < 0.0001$; CSS: $P < 0.0001$; Fig. 2c, d) and the combined cohort (OS: $P < 0.0001$; CSS: $P < 0.0001$; Fig. 2e, f). For the univariate Cox analysis, age at surgery, pathologic grade, TNM stage and TSR were identified as significant variables for OS in both cohorts. Similar results demonstrated that pathologic grade, TNM stage and TSR were identified as significant variables for CSS. Multivariate Cox analysis revealed that high TSR was a negative prognostic indicator of OS in the discovery cohort (HR: 1.537; 95% CI: 1.117–2.115; $P = 0.008$) and the validation cohort (HR: 2.134; 95% CI: 1.331–3.421; $P = 0.002$) (Supplementary Table S4). Analogously, multivariate Cox analysis revealed that TSR was independently predictive of CSS in the discovery cohort (HR: 1.835; 95% CI: 1.252–2.609; $P = 0.002$) and validation cohort.(HR: 2.060; 95% CI: 1.216–3.490; $P = 0.007$) (Supplementary Table S5).

### A higher TSR indicates inferior therapeutic responsiveness to ACT in Stage II–IV UTUC

Since patient characteristics might vary among patients treated with ACT vs. not treated with ACT in routine clinical practice, we used PSM to balance the baseline characteristics (Supplementary Table S6). As shown, before PSM, 6 out of 11 covariates were unbalanced between patients treated with ACT vs. not treated with ACT ($P < 0.1$) and our 1:4 PSM resulted in balanced covariates between the 2 groups ($P > 0.1$). Notably, the analysis of all the 291 patients showed ACT did not improve OS and CSS ($P = 0.16$, CSS: $P = 0.24$, Fig. 3a, b). However, among patients with stroma-low tumours, ACT treatment led to a superior OS and CSS (OS: $P = 0.011$; CSS: $P = 0.013$, Fig. 3c, d), whereas no ACT benefits were observed in the stroma-high group (OS: $P = 0.79$; CSS: $P = 0.59$; Fig. 3e, f). Collectively, these results suggested that TSR could identify UTUC patients who could benefit from ACT, and high tumour stroma levels potentially impeded ACT responsiveness.

### Stroma-high tumours were characterised by abundant cancer-associated fibroblasts

Cancer-associated fibroblasts (CAFs) are one of the most abundant and critical components of the tumour stroma. Interestingly, we found by differential expression analysis that CAF-related genes, such as TGFBI, TGFB3, CXCL12, VIM, FGF7, COL1A1, COL6A1, IL-6, were upregulated in the stroma-high group (Fig. 4a and Supplementary Table S7). Moreover, GSEA analysis revealed that CAF-related pathways, ECM receptor interaction and TGFβ signalling pathway, were the two significantly enriched pathways in the stroma-high group (Fig. 4b, c and Supplementary Table S8). Consistently, transcript data analysis using the MCP-counter algorithm indicated that CAFs were more abundant in the stroma-high group (Supplementary Fig. S2A). Our IHC analysis data confirmed that tumours in the stroma-high group showed a higher level of α-SMA$^+$ CAFs compared with the tumours in the stroma-low group (Fig. 4d and Supplementary Fig. S2B). Moreover,

**Table 1.** Associations between tumour-associated stroma and clinicopathological characteristics in patients with UTUC ($n = 1015$).

| Factors | Discovery set ($n = 710$) | | | Validation set ($n = 305$) | | |
|---|---|---|---|---|---|---|
| | Stroma-low ($n = 436$) | Stroma-high ($n = 274$) | *P* value | Stroma-low ($n = 186$) | Stroma-high ($n = 119$) | *P* value |
| Age at surgery (years) | | | 0.386 | | | 0.369 |
| Median (IQR) | 68.0 (60.0−75.0) | 67.0 (58.8−74.0) | | 68.0 (61.0−74.0) | 66.0 (59.0−74.5) | |
| Gender | | | 0.506 | | | 0.691 |
| Male | 226 (51.8%) | 135 (49.3%) | | 95 (51.1%) | 58 (48.7%) | |
| Female | 210 (48.2%) | 139 (50.7%) | | 91 (48.9%) | 61 (51.3%) | |
| Smoking | | | 0.319 | | | 0.347 |
| Never | 328 (75.2%) | 207 (75.5%) | | 134 (72.0%) | 98 (82.4%) | |
| Current/former | 63 (14.5%) | 49 (17.9%) | | 30 (16.1%) | 16 (13.4%) | |
| Unknown | 45 (10.3%) | 18 (6.6%) | | 22 (11.9%) | 5 (4.2%) | |
| Tumour location | | | 0.911 | | | **0.027** |
| Pelvis | 240 (55.0%) | 152 (55.5%) | | 110 (59.1%) | 55 (46.2%) | |
| Ureter | 196 (45.0%) | 122 (44.5%) | | 76 (40.9%) | 64 (53.8%) | |
| Left or right | | | 0.112 | | | 0.952 |
| Left | 232 (53.2%) | 129 (47.1%) | | 96 (51.6%) | 61 (51.3%) | |
| Right | 204 (46.8%) | 145 (52.9%) | | 90 (48.4%) | 58 (48.7%) | |
| Tumour size (cm) | | | 0.785 | | | 0.123 |
| <2 | 88 (20.2%) | 53 (19.3%) | | 36 (19.4%) | 15 (12.6%) | |
| ≥2 | 348 (79.8%) | 221 (80.7%) | | 150 (80.6%) | 104 (87.4%) | |
| Tumour multifocality | | | 0.529 | | | 0.677 |
| Unifocal | 363 (83.3%) | 233 (85.0%) | | 148 (79.6%) | 97 (81.5%) | |
| Multifocal | 73 (16.7%) | 41 (15.0%) | | 38 (20.4%) | 22 (18.5%) | |
| Pathologic grade | | | **<0.001** | | | **<0.001** |
| Low | 249 (57.1%) | 98 (35.8%) | | 99 (53.2%) | 38 (31.9%) | |
| High | 187 (42.9%) | 176 (64.2%) | | 87 (46.8%) | 81 (68.1%) | |
| Tumour stage | | | **<0.001** | | | **<0.001** |
| Ta-T2 | 333 (76.4%) | 136 (49.6%) | | 134 (72.0%) | 53 (44.5%) | |
| T3-T4 | 103 (23.6%) | 138 (50.4%) | | 52 (28.0%) | 66 (55.5%) | |
| Lymph node status | | | **<0.001** | | | 0.459 |
| N0 | 403 (92.4%) | 230 (83.9%) | | 169 (90.1%) | 105 (88.2%) | |
| N+ | 33 (7.6%) | 44 (16.1%) | | 17 (9.1%) | 14 (11.8%) | |
| TNM stage | | | **<0.001** | | | **<0.001** |
| I | 173 (39.7%) | 69 (25.2%) | | 76 (40.9%) | 31 (26.1%) | |
| II | 139 (31.9%) | 59 (21.5%) | | 50 (26.9%) | 17 (14.3%) | |
| III | 90 (20.6%) | 102 (37.2%) | | 43 (23.1%) | 56 (47.0%) | |
| IV | 34 (7.8%) | 44 (16.1%) | | 17 (9.1%) | 15 (12.6%) | |

*UTUC* upper tract urothelial carcinoma, *IQR* interquartile range, *TNM* tumour–node–metastasis
Bold values indicate statistical significance $p < 0.05$.

UTUC patients with a higher level of CAFs showed significantly shorter OS and CSS (OS: $P = 0.0051$; CSS: $P = 0.00059$, Fig. 4e, f).

### Tumour stroma modulates immunoevasive contexture of UTUC

Since the TME was correlated with survival outcomes and therapeutic responsiveness, we focused on investigating the potential impact of tumour stroma on immune contexture of UTUC. To systematically investigate whether tumour stroma was associated with immune infiltration in UTUC, we analysed the gene expression profiles to infer the density of the 13 immune cells using GSEA analysis (Supplementary Table S3). As shown in Fig. 5a, patients in different groups exhibited distinct immune infiltrate patterns. Specifically, significantly higher infiltration of tumour-associated macrophages (TAMs) was found in the stroma-high group (Fig. 5a). Consistently, our IHC analysis data confirmed that the infiltration of $CD68^+$ TAMs, as well as $CD206^+$ TAMs (M2-TAMs) were significantly higher in the stroma-high group ($P = 0.043$, $P = 0.025$, respectively, Fig. 5b). Besides, $CD66b^+$ tumour-infiltrating neutrophil and $Foxp3^+$ regulatory T cells (Tregs) infiltration were higher in stroma-high subgroup ($P = 0.011$, $P = 0.002$, respectively, Fig. 5b and Supplementary Fig. S3A, B).

To determine whether tumour stroma could impair the anti-tumour function of T cells, we further investigate the state of effector T cells in patients with UTUC. Our transcript data showed that T-cell infiltrated in stroma-high group exhibited exhausted phenotype with elevated expression of immune checkpoints (Fig. 5c). GSEA pathways were primarily enriched in "Exhausted $CD8^+$ T cell" (Fig. 5d and Supplementary Table S9). Multiplexed

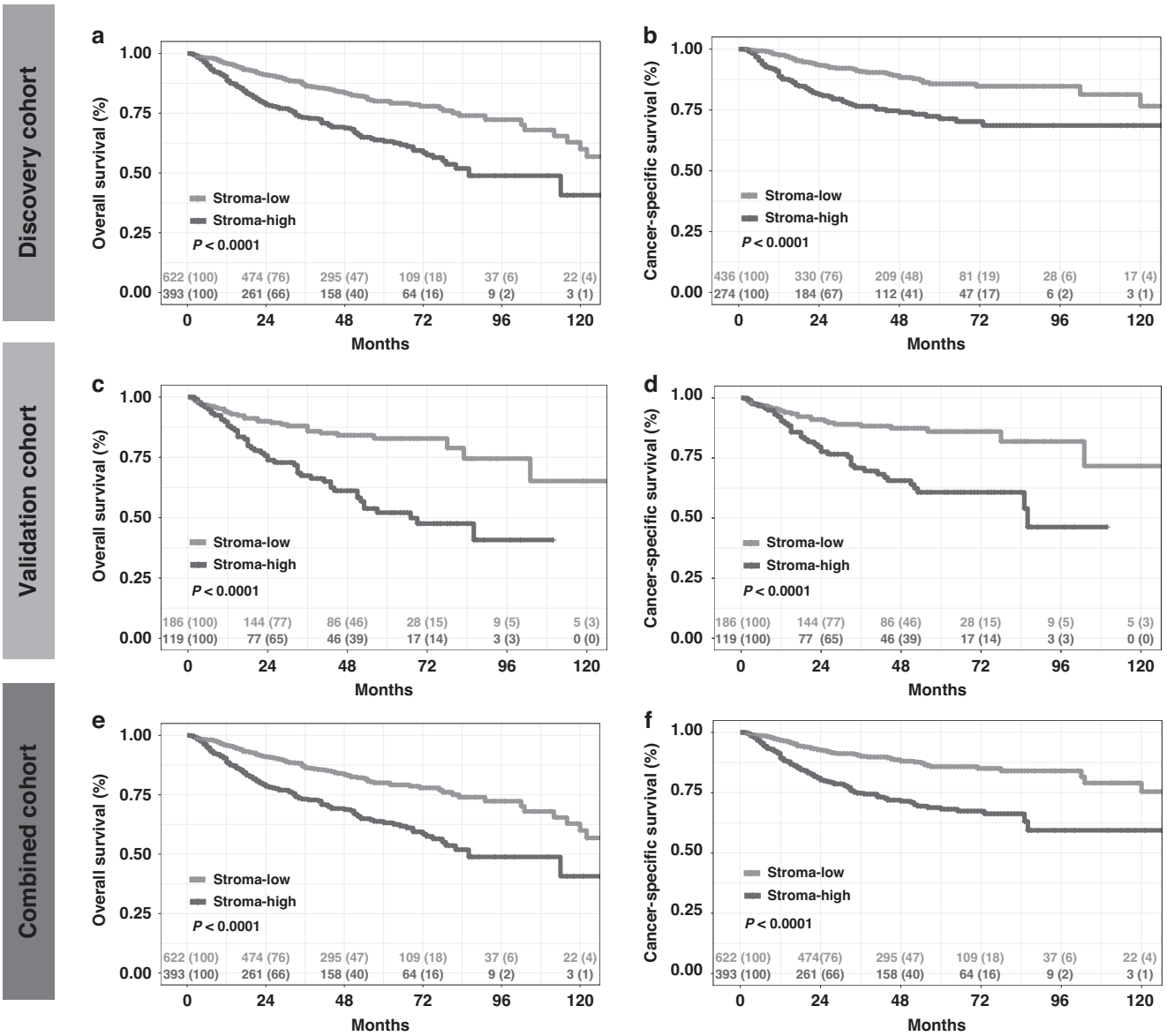


**Fig. 2 Association of the tumour-associated stroma with cancer survival outcome.** Kaplan–Meier analysis of overall survival (OS) and cancer-specific survival (CSS) of patients with UTUC stratified by tumour–stroma ratio (TSR) in the discovery cohort ($n = 710$) (**a**, **b**), validation cohort ($n = 305$) (**c**, **d**) and combined cohort ($n = 1015$) (**e**, **f**). *P* value was calculated by log-rank test.

immunofluorescence staining data confirmed that PD-1$^{+}$CD8$^{+}$ T cells and TIM-3$^{+}$CD8$^{+}$ T cells were significantly increased in stroma-high subgroup ($P < 0.001$ and $P = 0.024$, respectively; Fig. 5e–h). Thus, both the transcript and immunofluorescence data revealed that tumour stroma might shape the dysfunction of CD8$^{+}$ T cells in UTUC.

### Development and validation of TSR-based survival nomograms

Finally, we developed 3-year and 5-year OS and CSS nomogram models based on variables retained in the multivariate model (age at surgery, TSR, TNM stage and tumour pathologic grade) (Fig. 6a and Supplementary Fig. 4A). The calibration curve demonstrated favourable consistency between the nomogram-predicted 5-year OS or CSS and the observed 5-year OS or CSS (Supplementary Figs. 5A–C and 6A–C). The Harrell's concordance index (C-index) of our nomogram to predict OS was 0.690 (95% CI: 0.645–0.735) in the discovery cohort and 0.730 (95% CI: 0.671–0.79) in the validation cohort. While, the C-index for the CSS nomogram was 0.742 (95% CI: 0.718–0.766) in the discovery cohort, and 0.725 (95% CI: 0.695–0.759) in the validation cohort.

Based on the nomogram, the discovery cohort was categorised into the high-risk and low-risk groups, which revealed a significant difference in OS and CSS for the groups (Fig. 6b, $P < 0.001$; Supplementary Fig. 4b, $P < 0.001$). Similar results were obtained in the validation and combined cohorts. (Fig. 6c, d, both $P < 0.001$; Supplementary Fig. 4C, D, both $P < 0.001$). The AUC values of the nomogram predicting 5-year OS were 0.663 (95% CI: 0.602–0.724), 0.741 (95% CI: 0.664–0.819), and 0.684 (95% CI: 0.636–0.733) in the discovery, validation and combined cohorts, respectively. Moreover, the AUC values of the nomogram predicting 5-year CSS were 0.721 (95% CI: 0.657–0.785), 0.747 (95% CI: 0.662–0.831), and 0.730 (95% CI: 0.680–0.781) in the discovery, validation and combined cohorts, respectively. Improved prognostic accuracy was shown for OS and CSS compared to the TNM stage and TSR (Fig. 6e–g and Supplementary Fig. 4E–G). The decision curve analysis (DCA) curves in the discovery, validation and combined cohorts revealed

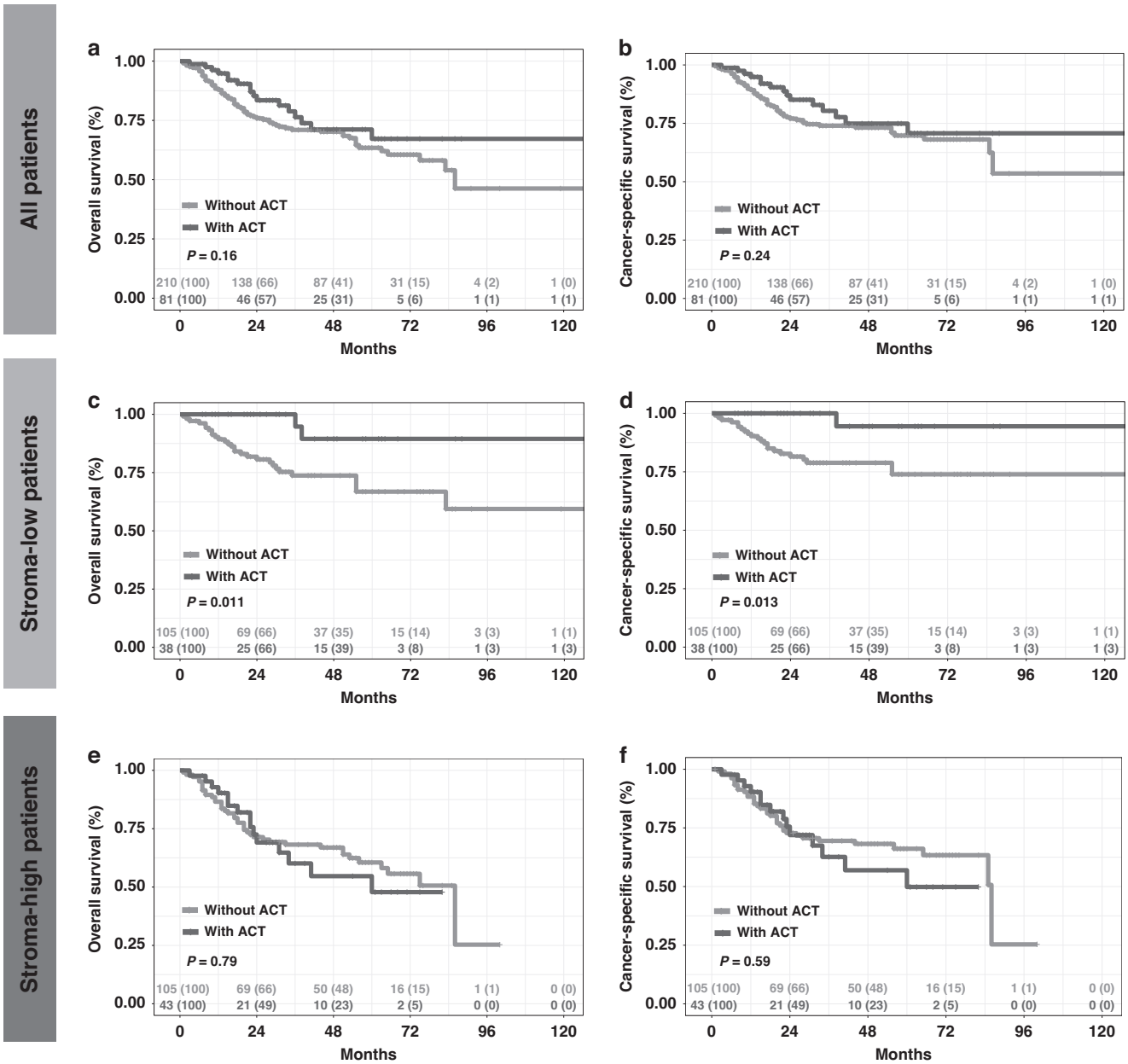


**Fig. 3 The relationship between tumour-associated stroma and benefit of adjuvant chemotherapy (ACT) in patients with Stage II–IV upper tract urothelial carcinoma (UTUC). a**, **b** Overall survival (OS) and cancer-specific survival (CSS) for Stage II–IV UTUC patients with ACT and without ACT. OS and CSS for Stage II–IV UTUC patients with ACT and without ACT in the stroma-low subgroup (**c**, **d**) and stroma-high subgroup (**e**, **f**). *P* value was calculated by log-rank test.

preferable positive net benefit and showed good clinical application potential (Supplementary Figs. 5D–F and 6D–F).

## DISCUSSION

Accurate risk stratification is crucial for the tailored ACT and follow-up strategies in patients with UTUC. In this study, we conducted a real-world study to investigate the prognostic role of the TSR in UTUC, termed TSU-01, using a large, nationwide cohort comprising over 1000 patients. Our study comprehensively demonstrated that the TSR is a highly reproducible, robust and independent prognostic factor in UTUC. This simple, routinely available biomarker adds important prognostic and predictive information to the current standard clinicopathological parameters of UTUC. To the best of our knowledge, this is the first study to investigate the role of TSR in patients with UTUC. Based on these findings, we constructed a high-performance prognostic model that integrated TME information to clinicopathological factors, which might help optimise the adjuvant strategies for UTUC patients.

Tumour-associated stroma, which directly surrounds tumour cells, is thought to be essential for tumour growth and progression [31]. Accumulating evidence shows that high TSR is associated with a worse cancer prognosis [14–16]. Consistently, we found that the TSR varied widely among different patients and high TSR correlated with aggressive clinicopathological features as well as poorer cancer survival. A promising prognostic value of TSR was observed in the validation cohort and it acted as an independent negative factor for survival for both cohorts, which further demonstrated the general applicability of this biomarker in all UTUC patients.

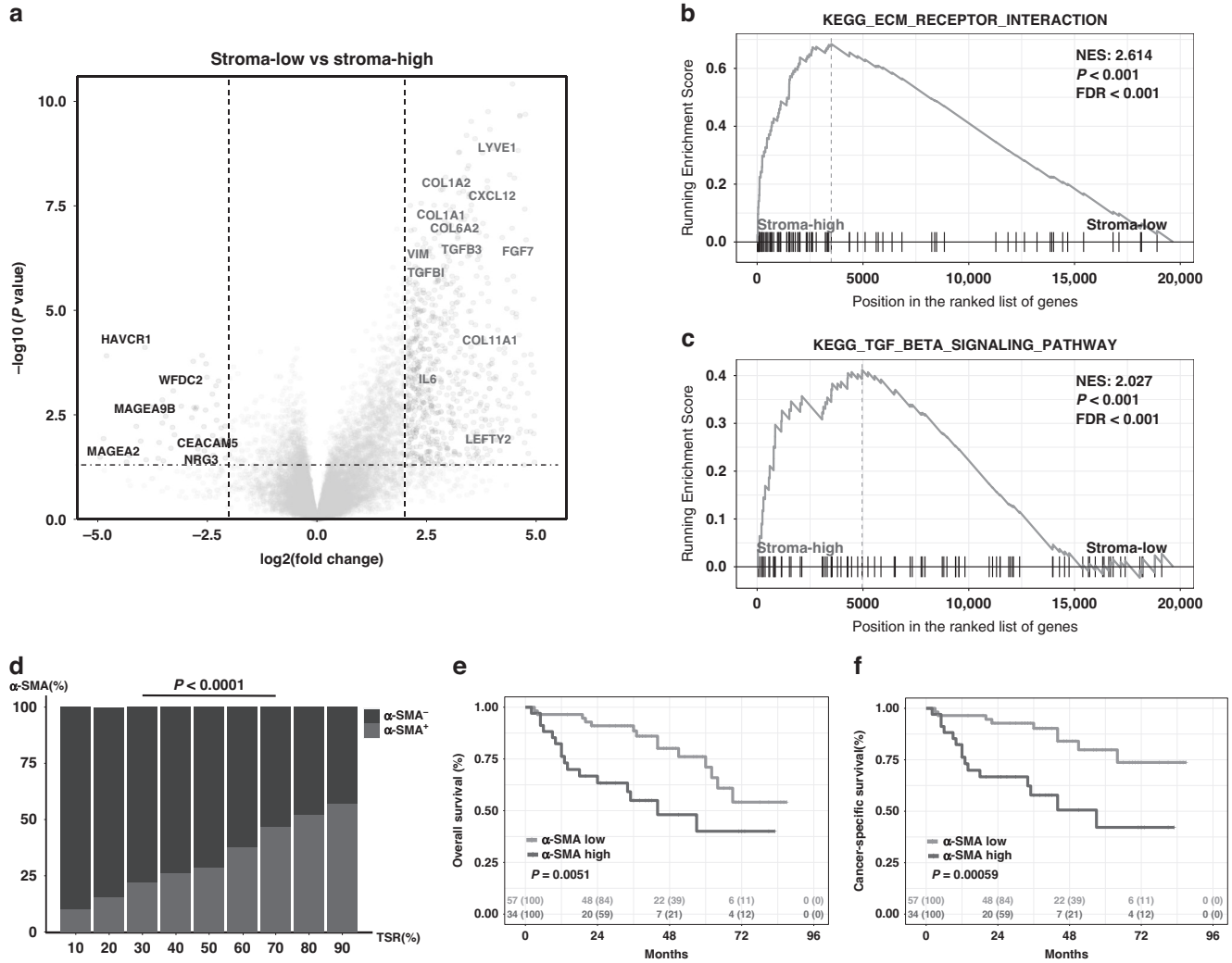


**Fig. 4 Stroma-high tumours were characterised by abundant cancer-associated fibroblasts (CAFs). a** Volcano plot showing the difference in RNA expression between stroma-high and stroma-low tumours. (Genes with fold change ≥2 and statistical significance are marked with red dots). **b**, **c** Gene Set Enrichment Analysis (GSEA) enrichment score curves of stroma-low vs. stroma-high tumours. **d** The distribution of low and high α-SMA expression in different tumour–stroma ratio (TSR) of patients with UTUC. Chi-square test was applied. **e**, **f** Overall survival (OS) and cancer-specific survival (CSS) of patients with low and high α-SMA expression in patients with UTUC.

A recent study proposed a new TSNM system by integrating the TSR into the TNM staging system of gastric cancer, which significantly improved the prediction accuracy for OS [32]. We hypothesised that the analysis of TSR and clinicopathologic characteristics could be combined to predict UTUC survival and could outperform the current TNM system. By constructing a prognostic nomogram, our study revealed that the TSR provided auxiliary information distinct from the TNM stage and histological grade system. Compared with the clinicopathologic characteristics, our nomogram significantly improve the predictive accuracy for cancer survival of patients with UTUC.

In current clinical practice, there is still no international consensus about the benefit of ACT for patients with UTUC after RNU [2]. Admittedly, the prospective study (POUT) demonstrated that adjuvant chemotherapy significantly improved disease-free survival in patients with locally advanced UTUC [2]. However, the updated outcomes demonstrated that adjuvant chemotherapy did not significantly improve the OS for the same cohort [33]. Therefore, efforts to accurately identify those patients who might benefit from ACT are urgently needed. Previous studies demonstrated that TSR might help clinicians with ACT strategies in other malignant tumours [34, 35]. Karpathiou et al. found that stroma-high tumours were an independent predictive factor for chemoresistance in patients with laryngeal and pharyngeal squamous cell carcinomas [36]. A more recent study demonstrated that the tumour–stroma proportion of ovarian carcinoma was associated with the eventual emergence of platinum chemoresistance [15]. Consistent with previous studies, although ACT did not show a survival advantage in all patients, patients with stroma-low tumours other than stroma-high ones, could benefit from ACT for UTUC.

Despite the recognition of the prognostic and predictive role of tumour stroma, the mechanism by which stroma affects disease progression in UTUC patients is poorly understood. It has been demonstrated that CAFs, which represent one of the major cellular components of the TME, are key players in tumorigenesis, tumour progression, angiogenesis and tumour invasion [18, 37, 38]. Not surprisingly, our results demonstrated that the stroma-high UTUCs have more CAFs, which could benefit more of the tumour growth supporting TME. Moreover, previous studies suggested that tumour stroma might influence immune cell recruitment and suppress the tumour immune response

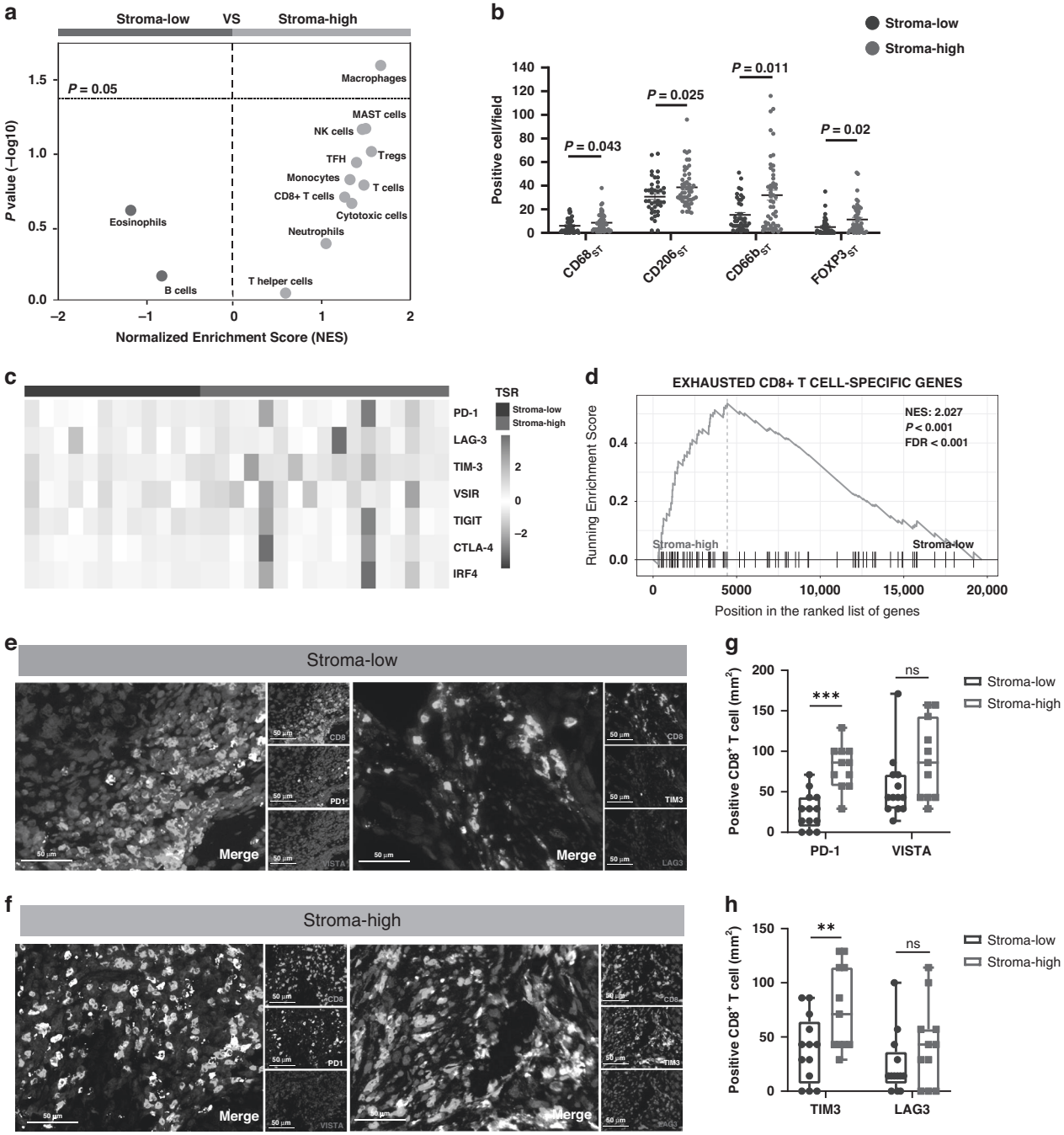


**Fig. 5 Characterisation of the immunoevasive tumour microenvironment in stroma-high tumours. a** Volcano plots for the enrichment of immune cell types for tumours with stroma-high and stroma-low tumours calculated based on the normalised enrichment score (NES) from the gene set enrichment analysis (GSEA). **b** Quantification analysis of CD68, CD206, CD66b, Foxp3 expression level between stroma-low and stroma-high tumours in UTUC. **c** Heatmap of exhaustion receptors and ligands genes expression of patients with UTUC stratified by tumour–stroma ratio (TSR). Expression was normalised via Z-score. **d** Enrichment of gene signatures of "$CD8^+$ T-cell exhaustion" was tested between stroma-low and stroma-high tumours by GSEA. **e**, **f** Representative immunofluorescence images of immune checkpoint expression (TIM-3/LAG-3/PD-1/VISTA) on $CD8^+$T cell (original magnification, ×200) in stroma-low and stroma-high tumours. **g**, **h** Percentage of TIM-$3^+$/LAG-$3^+$/PD-$1^+$/VISTA$^+$ $CD8^+$T cell in stroma-low and stroma-high tumours. Statistical analysis was performed with Mann–Whitney test.

[34, 39]. Thus, a better understanding of the inter-relationship between immune cells and tumour stroma, may help decide treatment strategies for the modulation of the immune response. We found that increasing proportion of stroma was associated with a pro-tumorigenic TME, represented by a high number of tumour-associated macrophages and exhausted T cells. Our study indicated that a highly tumour stroma-remodelled TME was characterised by immunoevasive contexture, which might promote adverse prognosis and reduction of the ACT benefit in patients with UTUC.

This study has several inherent limitations. First, the exploratory and retrospective design of this study may lead to a certain level of selection bias. For example, we did not randomly select patients for ACT and the sample size of patients receiving ACT in the cohort is not large enough to draw a definite conclusion. Second, TSR may be a useful biomarker for predicting the response to

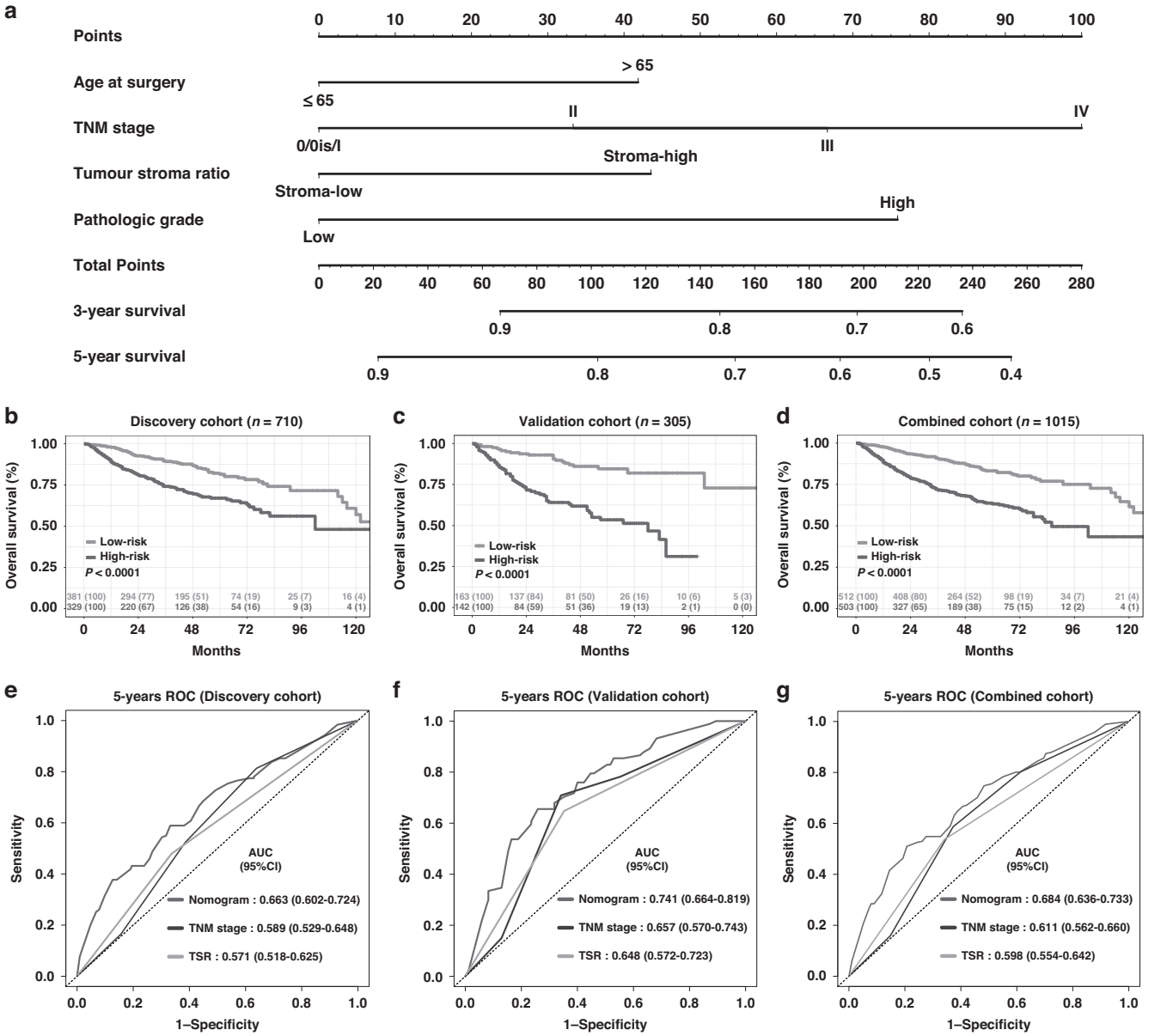


**Fig. 6 Construction of a TSR-based survival nomogram for upper tract urothelial carcinoma (UTUC). a** The multinomial nomogram for the prediction of 3-year and 5-year overall survival of UTUC patients. **b**–**d** Survival curves of patients with low-risk and high-risk groups based on TSR-based nomogram in the discovery cohort, validation cohort, and combined cohort. **e**–**g** The receiver operating characteristic (ROC) curve and the area under the curve (AUC) of the nomogram for 5-year OS in the discovery cohort, validation cohort and combined cohort.

immunotherapy, but further validation is needed in an anti-PD-1/PD-L1 immunotherapy UTUC cohort. Third, the mechanisms behind the association of the TSR with the immune response and tumour progression were not clearly elucidated. Therefore, further research is needed to delineate the interactions between tumour stroma and different immune cells. Despite these limitations, the TSR analysis can be performed by every pathologist with optimum reproducibility, and our nomogram has achieved a considerable prognostic performance. The TSR-based nomogram for UTUC warrants future application.

## DATA AVAILABILITY

The datasets used and/or analysed during the current study are available from the corresponding author on reasonable request.

## REFERENCES

1. Siegel RL, Miller KD, Jemal A. Cancer statistics, 2019. CA Cancer J Clin. 2019;69:7–34.
2. Birtle A, Johnson M, Chester J, Jones R, Dolling D, Bryan RT, et al. Adjuvant chemotherapy in upper tract urothelial carcinoma (the POUT trial): a phase 3, open-label, randomised controlled trial. Lancet. 2020;395:1268–77.
3. Lughezzani G, Burger M, Margulis V, Matin SF, Novara G, Roupret M, et al. Prognostic factors in upper urinary tract urothelial carcinomas: a comprehensive review of the current literature. Eur Urol. 2012;62:100–14.
4. Meng ZW, Pan W, Hong HJ, Chen JZ, Chen YL. Modified staging classification for intrahepatic cholangiocarcinoma based on the sixth and seventh editions of the AJCC/UICC TNM staging systems. Medicine. 2017;96:e7891.
5. Soukup V, Capoun O, Cohen D, Hernandez V, Babjuk M, Burger M, et al. Prognostic performance and reproducibility of the 1973 and 2004/2016 World Health Organization Grading Classification Systems in non-muscle-invasive bladder cancer: a European association of urology non-muscle invasive bladder cancer guidelines panel systematic review. Eur Urol 2017;72:801–13.

6. Necchi A, Lo Vullo S, Mariani L, Moschini M, Hendricksen K, Rink M, et al. Adjuvant chemotherapy after radical nephroureterectomy does not improve survival in patients with upper tract urothelial carcinoma: a joint study by the European Association of Urology-Young Academic Urologists and the Upper Tract Urothelial Carcinoma Collaboration. BJU Int. 2018;121:252–9.
7. Seisen T, Krasnow RE, Bellmunt J, Roupret M, Leow JJ, Lipsitz SR, et al. Effectiveness of adjuvant chemotherapy after radical nephroureterectomy for locally advanced and/or positive regional lymph node upper tract urothelial carcinoma. J Clin Oncol. 2017;35:852–60.
8. Quhal F, Mori K, Sari Motlagh R, Laukhtina E, Pradere B, Roupret M, et al. Efficacy of neoadjuvant and adjuvant chemotherapy for localized and locally advanced upper tract urothelial carcinoma: a systematic review and meta-analysis. Int J Clin Oncol. 2020;25:1037–54.
9. Tanaka N, Kikuchi E, Shirotake S, Kanao K, Matsumoto K, Kobayashi H, et al. The predictive value of C-reactive protein for prognosis in patients with upper tract urothelial carcinoma treated with radical nephroureterectomy: a multi-institutional study. Eur Urol. 2014;65:227–34.
10. Tanaka N, Kikuchi E, Kanao K, Matsumoto K, Shirotake S, Miyazaki Y, et al. A multi-institutional validation of the prognostic value of the neutrophil-to-lymphocyte ratio for upper tract urothelial carcinoma treated with radical nephroureterectomy. Ann Surg Oncol. 2014;21:4041–8.
11. Giraldo NA, Sanchez-Salas R, Peske JD, Vano Y, Becht E, Petitprez F, et al. The clinical role of the TME in solid cancer. Br J Cancer. 2019;120:45–53.
12. Xie HY, Shao ZM, Li DQ. Tumor microenvironment: driving forces and potential therapeutic targets for breast cancer metastasis. Chin J Cancer. 2017;36:36.
13. Park JH, McMillan DC, Edwards J, Horgan PG, Roxburgh CS. Comparison of the prognostic value of measures of the tumor inflammatory cell infiltrate and tumor-associated stroma in patients with primary operable colorectal cancer. Oncoimmunology. 2016;5:e1098801.
14. Liu J, Liu J, Li J, Chen Y, Guan X, Wu X, et al. Tumor-stroma ratio is an independent predictor for survival in early cervical carcinoma. Gynecol Oncol. 2014;132:81–6.
15. Lou E, Vogel RI, Hoostal S, Klein M, Linden MA, Teoh D, et al. Tumor-stroma proportion as a predictive biomarker of resistance to platinum-based chemotherapy in patients with ovarian cancer. JAMA Oncol. 2019;5:1222–4.
16. Huijbers A, Tollenaar RA, v Pelt GW, Zeestraten EC, Dutton S, McConkey CC, et al. The proportion of tumor-stroma as a strong prognosticator for stage II and III colon cancer patients: validation in the VICTOR trial. Ann Oncol. 2013;24:179–85.
17. Chen Y, Zhang L, Liu W, Liu X. Prognostic significance of the tumor-stroma ratio in epithelial ovarian cancer. Biomed Res Int. 2015;2015:589301.
18. Huang J, Zhang L, Wan D, Zhou L, Zheng S, Lin S, et al. Extracellular matrix and its therapeutic potential for cancer treatment. Signal Transduct Target Ther. 2021;6:153.
19. Idorn M, Olsen M, Halldorsdottir HR, Skadborg SK, Pedersen M, Hogdall C, et al. Improved migration of tumor ascites lymphocytes to ovarian cancer microenvironment by CXCR2 transduction. Oncoimmunology. 2018;7:e1412029.
20. Quail DF, Joyce JA. Microenvironmental regulation of tumor progression and metastasis. Nat Med. 2013;19:1423–37.
21. Xu B, Li XL, Ye F, Zhu XD, Shen YH, Huang C, et al. Development and validation of a nomogram based on perioperative factors to predict post-hepatectomy liver failure. J Clin Transl Hepatol. 2021;9:291–300.
22. Zhong W, Wang B, Yu H, Lin J, Xia K, Hou W, et al. Serum CCL27 predicts the response to Bacillus Calmette-Guerin immunotherapy in non-muscle-invasive bladder cancer. Oncoimmunology. 2020;9:1776060.
23. Chen J, Zhong W, Yang M, Hou W, Wang X, Xia K, et al. Development and validation of a PD-L1/PD-1/CD8 axis-based classifier to predict cancer survival of upper tract urothelial carcinoma after radical nephroureterectomy. Cancer Immunol Immunother. 2021;70:2657–68.
24. Cheng S, Zhong W, Xia K, Hong P, Lin R, Wang B, et al. Prognostic role of stromal tumor-infiltrating lymphocytes in locally advanced upper tract urothelial carcinoma: a retrospective multicenter study (TSU-02 study). Oncoimmunology. 2021;10:1861737.
25. Li T, Fu J, Zeng Z, Cohen D, Li J, Chen Q, et al. TIMER2.0 for analysis of tumor-infiltrating immune cells. Nucleic Acids Res. 2020;48:W509–W14.
26. Becht E, Giraldo NA, Lacroix L, Buttard B, Elarouci N, Petitprez F, et al. Estimating the population abundance of tissue-infiltrating immune and stromal cell populations using gene expression. Genome Biol. 2016;17:218.
27. Love MI, Huber W, Anders S. Moderated estimation of fold change and dispersion for RNA-seq data with DESeq2. Genome Biol. 2014;15:550.
28. Subramanian A, Tamayo P, Mootha V, Mukherjee S, Ebert B, Gillette M, et al. Gene set enrichment analysis: a knowledge-based approach for interpreting genome-wide expression profiles. 2005;102:15545–50.
29. Bindea G, Mlecnik B, Tosolini M, Kirilovsky A, Waldner M, Obenauf AC, et al. Spatiotemporal dynamics of intratumoral immune cells reveal the immune landscape in human cancer. Immunity. 2013;39:782–95.
30. Zheng C, Zheng L, Yoo JK, Guo H, Zhang Y, Guo X, et al. Landscape of infiltrating T cells in liver cancer revealed by single-cell sequencing. Cell. 2017;169:1342–56.e16
31. Pagès F, Mlecnik B, Marliot F, Bindea G, Ou F-S, Bifulco C, et al. International validation of the consensus Immunoscore for the classification of colon cancer: a prognostic and accuracy study. Lancet. 2018;391:2128–39.
32. Peng C, Liu J, Yang G, Li Y. The tumor-stromal ratio as a strong prognosticator for advanced gastric cancer patients: proposal of a new TSNM staging system. J Gastroenterol. 2018;53:606–17.
33. Birtle AJ, Chester JD, Jones RJ, Jenkins B, Johnson M, Catto JW, et al. Updated outcomes of POUT: a phase III randomized trial of peri-operative chemotherapy versus surveillance in upper tract urothelial cancer (UTUC). J Clin Oncol. 2021;39:455.
34. van Wyk HC, Roseweir A, Alexander P, Park JH, Horgan PG, McMillan DC, et al. The relationship between tumor budding, tumor microenvironment, and survival in patients with primary operable colorectal cancer. Ann Surg Oncol. 2019;26:4397–404.
35. Zunder SM, van Pelt GW, Gelderblom HJ, Mancao C, Putter H, Tollenaar RA, et al. Predictive potential of tumour-stroma ratio on benefit from adjuvant bevacizumab in high-risk stage II and stage III colon cancer. Br J Cancer. 2018;119:164–9.
36. Karpathiou G, Vieville M, Gavid M, Camy F, Dumollard JM, Magne N, et al. Prognostic significance of tumor budding, tumor-stroma ratio, cell nests size, and stroma type in laryngeal and pharyngeal squamous cell carcinomas. Head Neck. 2019;41:1918–27.
37. Hinshaw DC, Shevde LA. The tumor microenvironment innately modulates cancer progression. Cancer Res. 2019;79:4557–66.
38. Mhaidly R, Mechta-Grigoriou F. Role of cancer-associated fibroblast subpopulations in immune infiltration, as a new means of treatment in cancer. Immunol Rev. 2021;302:259–72.
39. Yoo SY, Park HE, Kim JH, Wen X, Jeong S, Cho NY, et al. Whole-slide image analysis reveals quantitative landscape of tumor-immune microenvironment in colorectal cancers. Clin Cancer Res. 2020;26:870–81.

## ACKNOWLEDGEMENTS

The authors would like to thank Dr. Qun He, from the Department of Pathology, Peking University First Hospital, for his assistance with IHC and IF score.

## AUTHOR CONTRIBUTIONS

LHX, WLZ, PH and CCL performed experiments, statistical analysis and drafted the manuscript. KX, MY, RCL and SDC analysed and interpretation of the data. BW, KX, MY and JYC provided technical and material support. LLM, XSL, LQZ and JH provided study supervision and revised the manuscript. JH and TXL designed the study.

## FUNDING

This study was supported by the National Natural Science Foundation of China (Grant Nos. 81825016, 81961128027, 81902586, 81772719, 81772728); Guangdong Provincial Natural Science Foundation (2021A1515011541); Guangdong Provincial Clinical Research Center for Urological Diseases (2020B1111170006); Key Laboratory of Malignant Tumour Gene Regulation and Target Therapy of Guangdong Higher Education Institutes (Grant No. KLB09001); Key Laboratory of Malignant Tumor Molecular Mechanism and Translational Medicine of Guangzhou Bureau of Science and Information Technology (Grant No. 013-163); The National Key Research and Development Program of China (Grant No. 2018YFA0902803); The Key Areas Research and Development Program of Guangdong (Grant No. 2018B010109006).

## ETHICS APPROVAL AND CONSENT TO PARTICIPATE

All patients signed an informed consent before surgery that permitted the usage of resected tumours and clinical profiles in research, under the condition of anonymity. The study was approved by the ethics committee of each institution (SYSEC-KY-KS-2022-32), and conducted in accordance with the Declaration of Helsinki. Signed written informed consent was obtained from all patients.

## CONSENT TO PUBLISH

Consent for publication was obtained from all participants.

## COMPETING INTERESTS

The authors declare no competing interests.

## ADDITIONAL INFORMATION

**Supplementary information** The online version contains supplementary material available at https://doi.org/10.1038/s41416-022-02049-1.

**Correspondence** and requests for materials should be addressed to Xuesong Li, Liqun Zhou, Jian Huang or Tianxin Lin.